Long-Term Performance of Electrodes Based on Vinyl Acetate Homo-Polymer Binder

Pier Paolo Prosini[a,*], Mariasole Di Carli[a], Livia Della Seta[a], Maria Carewska[a] and Ivan Fuso Nerini[b]

[a]*ENEA, Italian National Agency for New Technologies, Energy and Sustainable Economic Development, Casaccia Research Centre, Via Anguillarese 301, 00123 Santa Maria di Galeria, Rome, Italy*

[b]*VINAVIL SpA, via Valtellina, 63 - 20159 Milano, Italy*

Abstract: In this work we propose the use of a hydro-dispersible polymer such as the poly vinyl acetate as a binder for the production of electrodes for lithium-ion batteries. To increase the film forming properties of the polymer the poly vinyl was added with triacetin that acts as a plasticizer. The electrochemical stability of the polymer was tested by a polarizing electrode, formed by mixing the polymer with carbon. Subsequently, an electrode tape was prepared by using $LiNi_{0.5}Mn_{1.5}O_4$ as the active material and characterized by SEM, EDS and TGA. Lithium metal cells were assembled and tested to evaluate specific capacity, power and energy density at various discharge rates. The cycle life of the cell was evaluated by galvanostatic charge/discharge cycles. The tests showed that the electrodes prepared with PVA plasticized with triacetin have very good electrochemical performance in terms of capacity retention as a function of the discharge rate and the cycle number. Our work demonstrates that the use of triacetin to plasticize the PVA allows to increase the electrochemical stability of the electrode likely due to an improvement of the slurry filmability. The proposed method could represent a promising technology for the production of long-term performance lithium batteries.

Keywords: Poly vinyl acetate, triacetin, composite cathode, lithium battery, $LiNi_{0.5}Mn_{1.5}O_4$.

1. INTRODUCTION

The use of water dispersible or water soluble binders for the production of electrodes for lithium batteries is proving to be a very promising production technology [1-7]. This procedure combines the advantages of a low-cost of the polymer materials used as binders with an environmentally compatible electrode fabrication processes. Various water dispersible binders have been proposed in literature: carboxymethyl cellulose (CMC) [4,8], sodium-CMC [9], sodium polyacrylate [5], styrene-butadiene rubber/CMC [2,3], carboxymethyl chitosan [6], alginate [10], poly vinyl acetate [11,12]. These polymers have been used to bind various active materials working at low [3-5], medium [6,11] as well as high voltage [2,12]. Among others, spinel $LiNi_{0.5}Mn_{1.5}O_4$ material is one of the most promising and attractive cathode materials for next generation lithium-ion batteries because of its high voltage (4.7 V), acceptable stability, and good cycling performance [13]. To be compatible with high voltage cathode materials, the polymer used as the binder must have a superior electrochemical stability. In a previous work [12] it was showed that the poly vinyl acetate (PVA) can be used as the binder of a high voltage cathode based on $LiNi_{0.5}Mn_{1.5}O_4$ (LMNO) as

active material. In fact, despite the polymer showed a limited stability especially at very high voltage, the electrode cycled for several cycles with a good capacity retention. In this work, to better the filmability of the electrode slurry we added glycerol triacetate to the PVA. The glycerol triacetate (also known as triacetin) is the acetic acid ester of the glycerol. The triacetin is an additive used as plasticizer in several applications [14]. It is also used to modify the viscosity of liquid fuels [15]. At room temperature it is a colorless oily liquid. Its boiling point is 248 °C. Triacetin has a remarkable ability to increase the film forming properties of the polymer [16]. This effect could lead to a better adhesion of the particles of active material on the conductive filler and a better electrical contact between the latter and the current collecting substrate, accordingly, increasing the electrochemical stability of the electrode. The improved quality of the so obtained electrodes allowed us to test their long term performance by evaluating the capacity retention as a function of the discharge rate and the cycle number.

2. MATERIALS AND METHODS

2.1. Preparation of the Electrode Tape

To improve the filmability of the electrode 10 g of triacetin was added to 100 g of a 60 wt.% dispersion of PVA in water. 0.78 g of LMNO (Nanomyte SP-10, IN Corporation Somerset, NJ, USA) and 0.12 g of carbon (Super P, MMM Carbon, Belgium) were weighed and

*Address correspondence to this author at the ENEA, Italian National Agency for New Technologies, Energy and Sustainable Economic Development, Casaccia Research Centre, Via Anguillarese 301, 00123 Santa Maria di Galeria, Rome, Italy; Tel: +39.06.3048.6978; Fax: +39.06.3048.6357; E-mail: pierpaolo.prosini@enea.it

transferred to a grinder. The powders were mixed, by operating the mill for a few minutes. 8 g of water was added to 0.16 g of PVA added with triacetin in water, corresponding to 0.1 g of dry polymer. The diluted polymer dispersion was added to the powder mixture and the whole was mixed by operating the mill for a few minutes. The so obtained suspension was used to deposit a thin layer of the composite on a sheet of aluminum covering a surface of 81 cm^2. After drying in air at 90-100 °C, the procedure was repeated as many times as necessary to use the entire suspension. The thickness of the electrode tape ranged between 60 and 100 μm. The composition of the electrode tape was 78 wt.% LMNO, 10 wt.% PVA, and 12 wt.% carbon. Circular electrodes with a diameter of 12 mm were prepared by cutting out discs from the electrode tape. The weight of the electrodes ranged between 10.5 and 16.0 mg, corresponding to a specific load of active material between 9.3 and 14.1 mg cm^{-2}. Before the electrochemical characterization the electrodes were dried by heating under vacuum at 100 °C for 12 h. A similar procedure was used to prepare an electrode tape devoid of the active material. In this case 0.10 g of carbon were mixed with an aqueous dispersion of PVA (also containing triacetin) prepared by adding 8 g of water to 0.16 g of the 60 wt.% aqueous suspension. Even in this case, the mixture was used to deposit a thin layer of the composite on an aluminum sheet. After drying in air at 90-100 °C, the procedure was repeated up to consume the entire suspension. The polarizing electrode thus obtained was used to evaluate the electrochemical stability window.

2.2. Physico-Chemical Characterization of the Electrode Tape

The morphology and composition of the electrode tape were evaluated using a scanning electron microscope (SEM). The high magnification photomicrographs were obtained using a Jeol JSM-5510LV. The surface chemical composition was mapped by X-ray analysis of energy dispersive spectroscopy (EDS) with a IXRF EDS-2000 system. The samples were mounted directly on a carbon conductive double-sided tape. The material density was determined using a helium pycnometer (Micromeritics AccuPyc).

2.3. Thermal Characterization

Thermal stabilities were verified in nitrogen and air using a simultaneous TG-DTA (Q600 SDT, TA Instruments) equipped with the Thermal Solution

Software (version 1.4). The temperature was calibrated using the nickel Curie point as the reference. The mass was calibrated using the standard ceramic supplied with the instrument. Aluminum oxide of high purity was used as reference material. Open platinum crucibles (with a cross-section diameter of 0.32 cm) were used to contain the samples. The experiments were performed on samples with a weight ranged between 10 and 12 mg. The thermal stability was evaluated by heating the sample in air from room temperature up to 750 °C at a rate of 10 °C min^{-1}. The starting decomposition temperature was calculated from the thermal analysis software (Universal Analysis version 2.5) as the intersection between the baseline weight and the extrapolated tangent to the inflection point of the weight/temperature curve.

2.4. Electrochemical Characterization

The electrochemical stability of the polymer and the cycling properties of the electrodes were examined in 2032 coin-type cells. Lithium metal was used both as the counter and the reference electrode. A glass fiber was used as separator. A 1.0 M solution of LiPF$_6$ in a mixture 1:1 of ethylene carbonate/diethyl carbonate was used as the electrolyte. The electrode prepared without the active material was used to evaluate the electrochemical stability window of the polymer. This test was performed by applying an anodic voltage scan carried out at a rate of 0.1 mV s^{-1}. The performance of the batteries and their cycle life were evaluated automatically via a battery cycler (Maccor 4000). The handling of the materials, the preparation of the composite cathode, the assembly of the cells and their testing were performed at 20 °C in a dry room (R.H. <0.1% at 20 °C).

3. RESULTS AND DISCUSSION

3.1. Morphological Characterization

Figure **1** shows a low magnification image (x50) of the electrode surface. The area shown in the figure has an extension of about 4 mm^2. The electrode surface appears smooth and furrowed by deep grooves that seem to reach the aluminum substrate used as current collector. At higher magnification (x1000, Figure **2** upper left) the surface appears rough and grainy. The roughness is mainly due to the presence of numerous structures emerging from the electrode surface and formed by the aggregation of particles of the active material. Depressions and cavities can be observed around these structure. The EDS analysis (Figure **2**)
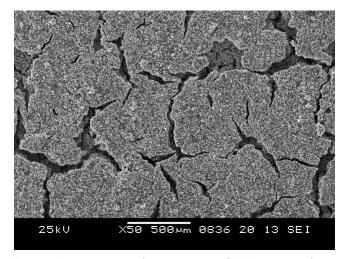
Figure 1: Low magnification (x50) SEM image of the electrode surface.

shows that, with the exception of the points where the depressions are present, both manganese and oxygen appear evenly distributed on the electrode surface. The study of the cross section (Figure **3**) shows that the electrode is quite compact and well adherent to the aluminum substrate. The electrode thickness, estimated through the image of the section, is around 103 μm. To evaluate the electrode porosity, the theoretical (d_t) and apparent (d_a) electrode densities

were calculated and used to evaluate the electrode porosity (p) as defined in eq. 1:

$$p = \frac{d_t - d_a}{d_t} 100 \qquad (1)$$

As previously reported [17] the theoretical density of a composite electrode can be calculated by considering the contribute of each single component of the composite electrode (eq. 2):

$$d_t = \frac{1}{\sum_{i=1}^{n} \frac{x_i}{d_{p(i)}}} 100 \qquad (2)$$

The density of the components was determined by a helium pycnometer and it is reported in Table **1** together with the percentage of the component in the electrode. By substituting the values in eq. 2 a theoretical density of 3.16 g cm^{-3} was calculated. The geometric density of the electrode was simply calculated as ratio between the mass and the volume of the sample. By considering the specific weight of the electrodes (10.5-16.0 mg), their area (1.13 cm^2) and thicknesses (68-103 μm), an apparent electrode density of 1.37 g cm^{-3} is calculated. The porosity of the
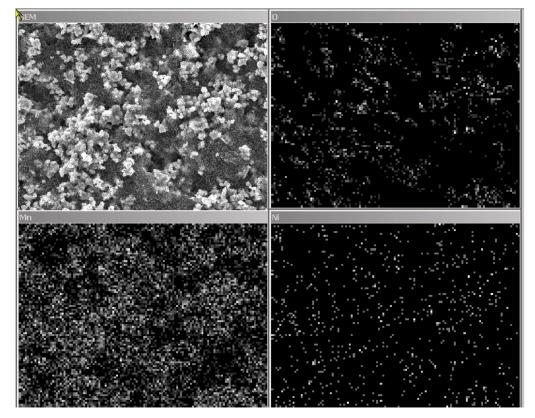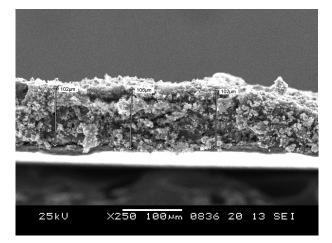

Figure 2: High magnification (x1000) SEM image at of the electrode surface and distribution of the various chemical components of the active material.

Table 1:   Density of the Materials and their Percentage by Weight in the Composite Electrode

Material	$LiNi_{0.5}Mn_{1.5}O_4$	Carbon	PVA
Density [g/cm^3]	4.45	2.13	1.18
Weight percent [%]	78	12	10

electrodes as calculated by using eq. 1 results to be 56.6%, higher than previously reported [12]. The higher value is probably related to the presence of the groves, as observed in Figure **1**, that determine an increase of empty spaces inside the electrode.
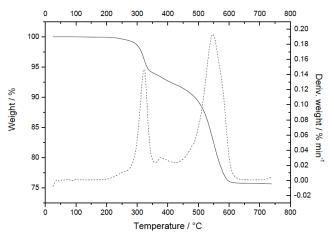

Figure 3: Medium magnification (x250) SEM image of the electrode cross section.

3.3. Thermal Characterization

It is known that the PVA degrades in two consecutive step when heated in air [18]. The first step, that extends up to 400 °C, leads to a weight loss of about 72% which corresponds to the de-acetylation of the polyolefinic chain. The second step starts around 450 °C. In this step the disintegration of the polyolefinic chain occurs and it results in the loss of almost the totality of the weight. The TGA profile and the corresponded weight derivative recorded during the decomposition of the PVA based electrode in air is shown in Figure **4**. The weight remains almost constant up to 200 °C. At around 227 °C the weight starts to decrease and a decomposition peak is observed between 280 and 360 °C with a maximum centered at 321 °C. According with the literature results, this peak can be ascribed to the loss of acetic acid. With respect to pure PVA the de-acetylation of the polyolefinic chain occurs at lower temperature. The second degradation step, corresponding to the disintegration of the polyolefinic chain, begins around 450 °C and ends at 600 °C with a maximum centered at 550 °C. In this step the carbon black introduced into the electrode
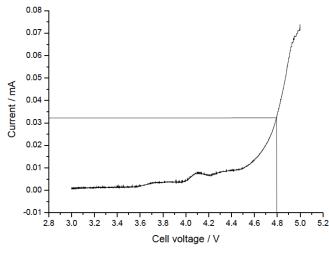
tape to increase the electric conductivity is also burned. The total weight loss is about 24 wt.%, slightly higher than the sum of the weight percentage of the polymer (10 %) and the carbon (12 %). This difference can be ascribed to the presence of a small amount of triacetin that was not completely removed during the heating treatment under vacuum.

Figure 4: Thermogravimetry (continuous line) and differential thermal analysis (dashed line) for the electrode based on PVA conducted from room temperature up to 750 °C at a rate of 10 °C min^{-1} in air.
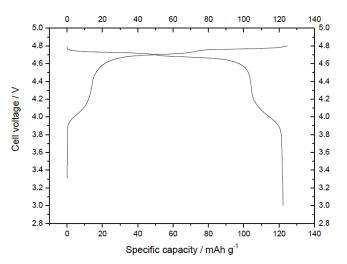
3.4. Electrochemical Characterization

Figure **5** shows the result of the test used to evaluate the electrochemical stability window of PVA. This measure has been borrowed from a similar procedure used to evaluate the stability of polymer electrolytes [19]. The test consists in applying a voltammetric scan in a lithium cell made with a polarizing electrode, containing only the carbon black and the polymer binder. The cell voltage was brought from the open circuit voltage (OVC) toward higher voltages and the current flowing through the cell was measured. Figure **5** reports the current flow as function of the applied voltage: the current flow remains very low, a fraction of μA, until the cell voltage reached 4.0 V. At higher voltages, a current of moderate intensity begins to flow through the cell. This indicates the occurrence of an anodic reaction at the inert electrode, most likely due to the oxidation of the anion. However, the value of the current remains very low (about 8 μA
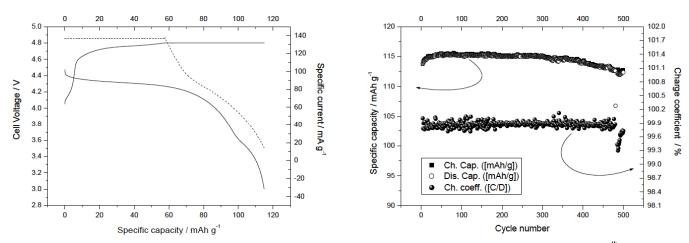
Figure 5: Polarization curve of a lithium cell containing a composite electrode containing a mixture of carbon and PVA (50%).

at 4.5 V) thus indicating a low reaction rate. Finally, at higher cell polarization (V> 4.5 V), the current starts to increase. When the cell voltage reaches the value of 4.8 V (the typical end charge voltage condition used to charge LMNO based cells) the current flowing into the system was about 32 μA. This low value confirms that it is possible to use the PVA as a binder of high voltage electrode materials without decreasing the Coulombic efficiency. To confirm this assumption a cell was assembled and cycled galvanostatically at C/10 rate between 4.8 and 3.0 V. Figure **6** shows the first cycle charge/discharge voltage profiles for the cell. In charge it is possible to observe a small plateau at 4.1 V, corresponding to the oxidation of Mn^{3+} to Mn^{4+}, and a larger one at 4.7 V related to the oxidation of Ni^{2+} to Ni^{4+} [20]. The specific capacity calculated at the end of the charge was about 124 mAh g^{-1} (this value was based on the weight of the active material in the electrode). In the following discharge the two plateaus are also observed with a small hysteresis in the voltage values. At the end of the discharge the specific capacity was about 122 mAh g^{-1}. Therefore the cell behaves in a reversible manner with a Coulombic efficiency higher than 98%. To evaluate the electrode cyclability the cell was galvanostatically charged at 1C rate up to 4.8 V, followed by a potentiostatic charging at 4.8 V until the current decreased to a value equal to C/10 rate (top-off mode). Figure **7** on the left shows the voltage and current profiles of a typical cycle of charge and discharge (in particular the 25th cycle). In charge the voltage reaches the top-off value after storing about 50% of the total capacity, being the remaining part of the charge stored during the potentiostatic step. In this step it is possible to observe, in the specific current profile, an inflection localized at around 80 mAh g^{-1}.

Before the inflection the specific current rapidly drops decreasing from 137 to about 80 mA g^{-1}. After reaching the inflection point the current continues to decrease more slowly until to reach the end charge condition (current lower than 13 mA g^{-1}). At this stage the total accumulated charge is 114 mAh g^{-1}. The initial voltage in the subsequent discharge step, conducted at 3C rate, is strongly affected by the high value of the discharge current: the cell voltage, immediately after the charging process, falls down to 4.47 V. Subsequently, the cell voltage reaches a plateau value centered at 4.31 V during which about 70% of the accumulated charge is released. Then the voltage drops to 3.5 V where the remaining part of the capacity is released, before to reach 3.0 V which corresponds to the end discharge condition. The discharge specific capacity was 113 mAh g^{-1}, practically more than 98% of the accumulated capacity in the previous charge step. Figure **7** on the right shows the variation of the specific capacity as a function of the number of cycles. The specific capacity slightly tends to increase during the first cycles reaching a value of 115 mAh g^{-1} at the 50th cycle. In the following cycles the cell presents no capacity loss so that the capacity is maintained unchanged during the subsequent cycles. After 300 cycles a very low capacity fade began to affect the cell. Notwithstanding, the capacity recorded after 500 deep charge/discharge cycles was as high as 112 mAh g^{-1}. The capacity retention with respect to the maximum capacity exhibited at the 50th cycle was 97.4%. Very impressive was also the value of the charge coefficient (defined as the percentage of the discharge capacity with respect to the capacity accumulated during the previous charge cycle): the charge coefficient remained higher than 99.8% for over 450 cycles. It is well known
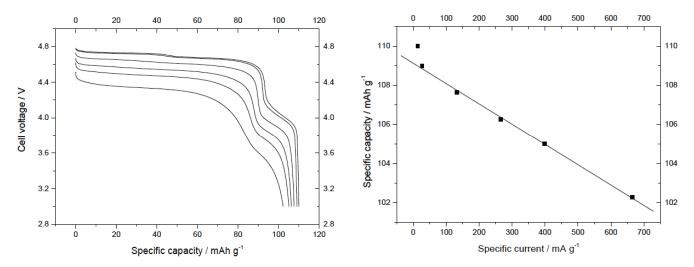

Figure 6: Charge and discharge profiles for the first cycle of a lithium / $LiNi_{0.5}Mn_{1.5}O_4$ cell carried out at C/10 rate.

Figure 7: Left: voltage (solid line) and current (dot line) profiles as a function of the specific capacity during the 25th cycle. Right: variation of the specific capacity and the charge coefficient as a function of the cycle number.

that the mechanical failure at the electrode interfaces (electrode/current collector and binder/particle interfaces) leads to particle isolation and electrode delamination, which has been regarded as one of the main reasons for the capacity decay and cell failure of lithium-ion batteries [21]. The high capacity retention shown by the PVA-based electrode is probably related to the high flexibility offered by the binder that allows to tolerate a greater movement of the active material while avoiding the occurrence of the detachment from the carbon particles or from the conductive current collector.
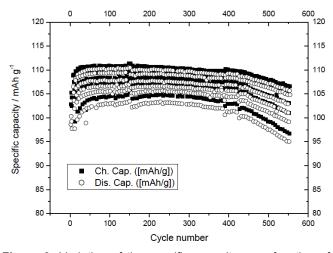
To evaluate the effect of the discharge current on the specific capacity, the electrode was cycled at various discharge currents, corresponding to the discharge rate of C/10, C/5, 1C, 2C, 3C, and 5C. The charge was performed galvanostatically at C rate up to 4.8 V, followed by a potentiostatic charging at 4.8 V

until the current decreases to a value equal to C/10 rate. Figure **8** on the left shows the discharge voltage profiles at the various discharge currents. It is possible to observe that the electrode based on PVA is able to support very high discharge currents while still maintaining most of its capacity. The discharged capacity seems almost insensitive to the variations in current: the electrode provides about 93% of the C/10 rated capacity when discharged at current 50 times higher (5C rate). This result may be related to a low electrode resistance probably due to a better adhesion of the active material with the carbon, a phenomenon that leads to an improvement of performance even at a high discharge rates. To evaluate the power response of the electrochemical system a method previously proposed in literature [22-23] was employed. The method is based on the calculation of a parameter k (in hours) defined by the equation:

Figure 8: Left: voltage profiles as a function of the specific capacity exhibited at various discharge currents corresponding to C/10, C/5, 1C, 2C, 3C and 5C rate. Right: variation of the specific current as a function of the specific power.

$$Q = Q^0 - k * I_m \qquad (4)$$

where Q [mAh g^{-1}] is the specific capacity exhibited at the specific current I_m [mA g^{-1}] (the discharge current divided by the mass of the active material in the electrode), and Q^0 [mAh g^{-1}] is the theoretical specific capacity (or the specific capacity exhibited at the lower discharge rate): the greater is the k parameter the worst is the electrode performance in terms of power. Figure **8** on the right shows the specific capacity as a function of the specific current. A linear correlation is found for discharge currents exceeding the C/10 rate. From the figure it is possible to extrapolate the value of the parameter k that has been calculated to be 0.01 h. This value is much lower than that found for LiFePO$_4$ electrodes and confirms the good current response of the electrodes prepared using PVA as a binder. Figure **9** shows the specific capacity as a function of the cycle number for the cell cycled at various discharge rates. Also in this case it is possible to observe a high capacity retention: the cell cycled for 400 cycles without any capacity loss. During the following 100 cycles a slight capacity fade affected the electrode. Anyway, the electrode performance is still more than enough even after 550 deep discharge cycles.

Figure 9: Variation of the specific capacity as a function of the cycle number at various discharge currents corresponding to C/10, C/5, 1C, 2C, 3C and 5C rate.

4. CONCLUSIONS

In this work, it has been shown that triacetic-based PVA electrodes have high electrochemical stability to allow them to be used with high-voltage materials such as LMNO. The calculated theoretical and apparent density show that the electrode has a high porosity. The electrode was used to build a cell where lithium metal acted as the anode. The cell was able of cycling for 500 cycles with good capacity retention and a surprising Coulombic efficiency of 99.8%. The electrode performance is almost insensitive to changes in current. The electrode is able to provide 93% of the capacity exhibited at C/10 when discharged at current 50 times higher. The value of the k parameter, that characterizes the power response of the system, is calculated to be 0.01 hours. This result may be related to the low electrode resistance due to a better adhesion of the active material with the carbon, a phenomenon that leads to an improvement of performance even at a high discharge rate.

ACKNOWLEDGMENTS

REFERENCES

[1]   Wood DL III, Li J, Daniel C. Prospects for reducing the processing cost of lithium ion batteries. J Power Sources 2015; 275: 234-242.
https://doi.org/10.1016/j.jpowsour.2014.11.019

[2]   Yabuuchi N, Kinoshita Y, Misaki K, Natsuyama T, Komaba S. Electrochemical Properties of LiCoO2 Electrodes with Latex Binders on High-Voltage Exposure. J Electrochem Soc 2015; 162: A538-A544.

[3]   He M, Yuan L-X, Zhang W-X, Hu X-L, Huang Y-H. Enhanced Cyclability for Sulfur Cathode Achieved by a Water-Soluble Binder. J Phys Chem C 2011; 115: 15703-15709.
https://doi.org/10.1021/jp2043416

[4]   Mancini M, Nobili F, Tossici R, Mehrens MW, Marassi R. High performance, environmentally friendly and low cost anodes for lithium-ion battery based on TiO2 anatase and water soluble binder carboxymethyl cellulose. J Power Sources 2011; 196: 9665-9671.
https://doi.org/10.1016/j.jpowsour.2011.07.028

[5]   Komaba S, Yabuuchi N, Ozeki T, Han Z-J, Shimomura K, Yui H, Katayama Y, Miura T. Comparative Study of Sodium Polyacrylate and Poly(vinylidene fluoride) as Binders for High Capacity Si-Graphite Composite Negative Electrodes in Li-Ion Batteries. J Phys Chem C 2012; 116: 1380-1389.
https://doi.org/10.1021/jp204817h

[6]   Sun M, Zhong H, Jiao S, Shao H, Zhang L. Investigation on Carboxymethyl Chitosan as New Water Soluble Binder for LiFePO4 Cathode in Li-Ion Batteries. Electrochim Acta 2014; 127: 239-244.
https://doi.org/10.1016/j.electacta.2014.02.027

[7]   Klamor S, Schröder M, Brunklaus G, Niehoff P, Berkemeier F, Schappacher FM, Winter M. On the interaction of water-soluble binders and nano silicon particles: alternative binder towards increased cycling stability at elevated temperatures. Phys Chem Chem Phys 2015; 175: 632-5641.
https://doi.org/10.1039/C4CP04090B

[8]   Qiu L, Shao Z, Wang D, Wang F, Wang J. Novel polymer Li-ion binder carboxymethyl cellulose derivative enhanced electrochemical performance for Li-ion batteries. Carbohydr Polym 2014; 112: 532-538.
https://doi.org/10.1016/j.carbpol.2014.06.034

[9]   Doberdo I, Löffler N, Laszczynski N, Cericola D, Penazzi N, Bodoardo S, Kim G-T, Passerini S. Enabling aqueous binders for lithium battery cathodes - Carbon coating of

aluminum current collector. J Power Sources 2014; 248: 1000-1006.
https://doi.org/10.1016/j.jpowsour.2013.10.039

[10] Soeda K, Yamagata M, Ishikawa M. Outstanding features of alginate-based gel electrolyte with ionic liquid for electric double layer capacitors. ECS Trans 2015; 64: 13-22.
https://doi.org/10.1149/06418.0013ecst

[11] Prosini PP, Cento C, Carewska M, Masci A. Poly vinyl acetate used as a binder for the fabrication of a LiFePO4-based composite cathode for lithium-ion batteries. Solid State Ionics 2015; 274: 34-39.
https://doi.org/10.1016/j.ssi.2015.02.012

[12] Prosini PP, Carewska M, Masci A. A high voltage cathode prepared by using polyvinyl acetate as a binder. Solid State Ionics 2015; 274: 88-93.
https://doi.org/10.1016/j.ssi.2015.03.008

[13] Santhanam R, Rambabu B. Research progress in high voltage spinel LiNi0.5Mn1.5O4 material. J Power Sources 2010; 195: 5442-5451.
https://doi.org/10.1016/j.jpowsour.2010.03.067

[14] Hasabnis A, Mahajani S. Entrainer-based reactive distillation for esterification of glycerol with acetic acid. Ind Eng Chem Res 2010; 49: 9058-9067.
https://doi.org/10.1021/ie100937p

[15] Rahmat N, Abdullah AZ, Mohamed AR. Recent progress on innovative and potential technologies for glycerol transformation into fuel additives: a critical review. Renew Sust Energ Rev 2010; 14: 987-1000.
https://doi.org/10.1016/j.rser.2009.11.010

[16] Zhu J, Li X, Huang C, Chen L, Li L. Plasticization effect of triacetin on structure and properties of starch ester film. Carbohyd Polym 2013; 94: 874-881.
https://doi.org/10.1016/j.carbpol.2013.02.020

[17] Appetecchi GB, Carewska M, Alessandrini F, Prosini PP, Passerini S. Characterization of PEO-based composite cathodes - I. Morphological, thermal, mechanical, and electrical properties. J Electrochem Soc 2000; 147: 451-459.
https://doi.org/10.1149/1.1393217

[18] Uyar T, Tonelli AE, Hacaloğlu J. Thermal degradation of polycarbonate, poly(vinyl acetate) and their blends. Polym Degrad Stab 2006; 91: 2960-2967.
https://doi.org/10.1016/j.polymdegradstab.2006.08.028

[19] Yuca N, Zhao H, Song X, Dogdu MF, Yuan W, Fu Y, Battaglia VS, Xiao X, Liu GA. Systematic Investigation of Polymer Binder Flexibility on the Electrode Performance of Lithium-Ion Batteries. ACS Appl Mater Interfaces 2014; 6: 17111-17118.
https://doi.org/10.1021/am504736y

[20] Zhong Q, Bonakdarpour A, Zhang M, Gao Y, Dahn JR. Synthesis and Electrochemistry of $LiNi_xMn_{2-x}O_4$. J Electrochem Soc 1997; 144: 205-213.
https://doi.org/10.1149/1.1837386

[21] Sylla S, Sanchez J-Y, Armand M. Electrochemical study of linear and cross linked POE-based polymer electrolytes. Electrochim Acta 1992; 37: 1699-1701.
https://doi.org/10.1016/0013-4686(92)80141-8

[22] Prosini PP. Modelling the voltage profile for LiFePO4. J Electrochem Soc 2005; 152: A1925-A1929.

[23] Fongy C, Gaillot AC, Jouanneau S, Guyomard D, Lestriez B. Ionic vs Electronic Power Limitations and Analysis of the Fraction of Wired Grains in LiFePO4 Composite Electrodes. J Electrochem Soc 2010; 157: A885-A891.